PROCEEDINGS, Twentieth Workshop on Geothermal Reservoir Engineering
Stanford University, Stanford, California, January 24-26 1995
SGP-TR-150

# THERMODYNAMIC TRANSIENT BEHAVIOR OF A GEOTHERMAL FRACTURE

Ascencio,F. (1), Samaniego,F. (2), Cinco-Ley,H. (2), Rivera,J. (2)
(1) Escuela de Ingeniería Mecánica. Universidad Michoacana.
Edificio W, Ciudad Universitaria. Morelia, Mich., México. CP 58060
(2) Universidad Nacional de México.

## ABSTRACT

This paper presents a space integrated zero dimensional model that describes the thermodynamic behavior of a geothermal fracture undergoing exploitation. The main assumptions involved are: fluid and energy entering the fracture come from the surrounding matrix, fracture of infinite conductivity, and that the steam and water phases are gravitationally segregated and in thermodynamic equilibrium. The nonlinear equations of mass and energy conservation are numerically solved. A sensitivity analysis on the main parameters that affect this problem was carried out. Water recharge is described by a linear infinite aquifer, and heat flow from the matrix to the fluid was also considered by means of a linear infinite system. The behavior of the system is clearly described for conditions of exploitation in the steam, in the water, or mixed completion in both steam and water zones.

## INTRODUCTION

The main aim of reservoir engineering is to determine the optimum exploitation conditions of a reservoir. Currently mathematical modeling plays a very important role in accomplishing this task. In a general sense these models consists of a set of nonlinear partial differential equations, relating the conservation of mass and energy. The use of reservoir simulation would allow the consideration of all production schemes considered as viable; thus, after proper economic analysis the optimum exploitation procedure for the reservoir can be determined.

Historically there have been two types of models used to predict the behavior of a reservoir; the zero dimensional models (ZDM) and the distributed parameters models (DPM). Zero dimensional models consider that rock and fluid properties are uniform and independent of the position in the reservoir. Two approaches for the consideration of these ZDM models have been presented in the literature. The first uses the classical visualization of the integrated material balance equation (Shilthius, 1936; Craft and Hawkins, 1959; Whiting and Ramey, 1969; Brigham and Morrow, 1977; Brigham and Neri, 1980; Grant, 1977; Sorey and Fradkin, 1979; Castanier et al., 1980). The second approach uses a space integrated version of the partial differential equations of the distributed parameters models. These type of models have been previously described in the petroleum engineering literature (Muskat, 1945; Raghavan, 1994). In the application of these models to geothermal reservoir engineering, time is the independent variable and the model is composed of ordinary differential equations for the mass conservation of vapor and water, and for energy conservation.

The complex distributed parameters models (Brownell et al., 1977; Garg et al., 1975; Garg and Pritchet, 1977; Faust and Mercer, 1979,a,b; Pruess 1983, 1987, 1988) consider the spatial and time distribution of the formation and fluid properties. The equations for the conservation of mass and energy are discretized in space and time and are numerically solved.

The purpose of this paper is to present a space integrated zero dimensional model (SIZDM), for the description of the thermodynamic behavior of a geothermal fracture undergoing exploitation. The main assumptions involved are: recharge fluid enters the fracture through the original liquid level, energy entering the fracture comes from the surrounding matrix, fracture of infinite conductivity, and that the vapor and water phases are gravitationally segregated and in thermodynamic equilibrium.

# MATHEMATICAL MODEL

We consider an infinite conductivity geothermal fracture (ICGF), with gravity segregated steam and water in thermodynamic equilibrium, as shown in Fig. 1. Applying the principles of mass and energy balances we obtain the following set of differential equations:

*Mass conservation:*

$$\phi_f bL\frac{d}{dt}(\rho_w z_l + \rho_s(z_t - z_l)) = w_r - w_{wp} - w_{sp} \quad (1)$$

The water recharge $w_r$ term in Eq. 1 represents the natural recharge to the fracture, which can be expressed through the convolution integral given by Eq. 2:

$$w_r = \int_0^t \frac{\partial \Delta p(\tau)}{\partial \tau} w_1(t-\tau)d\tau \quad (2)$$

In Eq. 2 $w_1$ represents the influence function for the recharge system, or in other words is a unit pressure drop water recharge response. Considering a linear recharge system, the influence function is given by Eq. 3 (Miller, 1962; Nabor and Barham, 1964):

$$w_1 = \phi_r \rho_r b z_{l,t=0}\ c_t\sqrt{\frac{k}{\pi\phi_r\mu_r c_t t}} \quad (3)$$

*Energy conservation:*

$$\phi_f bL\frac{d}{dt}(\frac{(1-\phi_f)}{\phi_f}\rho_{sR}c_{sR}z_t T + \rho_w u_w z_l + \rho_s u_s(z_t - z_l))$$

$$= w_r h_r - w_{wp}h_w - w_{sp}h_s + q \quad (4)$$

Eq. 4 assumes that within the fracture thermodynamic equilibrium prevails between the steam, water, and the rock.

Similary to the previous discussion on recharge mass flow, the heat rate toward the fracture $q$ can be expressed by Eq. 5:

$$q = \int_0^t \frac{\partial \Delta T(\tau)}{\partial \tau} q_1(t-\tau)d\tau \quad (5)$$

Considering that this rate comes through the two fracture faces, under linear flow conditions, the heat influence function is given by Eq. 6 (Carslaw and Jaeger, 1959):

$$q_1 = 2z_t L\sqrt{\frac{\rho_R c_R \kappa_R}{\pi t}} \quad (6)$$

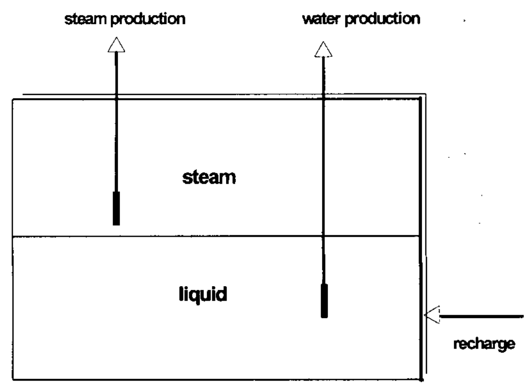


Fig. 1. Infinite conductivity geothermal fracture (ICGF).

# NUMERICAL SOLUTION

The nonlinear system of equations given by expressions 1 and 4 was solved through an iterative numerical procedure, briefly described as follows:

1. The fracture temperature in an unknown integration $\Delta t$ time step decreases in $\Delta T = T_i - T_{i-1}$, where $i$ refers to the time level. Thus, in accordance to this consideration, the thermodynamic properties of the steam and water phases at saturation conditions can be determined. It is considered that $T_0$ and $p_0$ are the temperature and pressure of the fracture at initial conditions.

2. Eqs. 1 and 4 are discretized on time and solved for the unknowns liquid level $z_{l,i}^k$ and the time step $\Delta t_i^k$, where $k$ is the iteration level.

$$a_m z_{l,i}^k - b_m \Delta t_i^k = c_m \quad (7)$$

$$a_e z_{l,i}^k - b_e \Delta t_i^k = c_e \quad (8)$$

The coefficient in these Eqs. 7 and 8 are defined by the following expressions:

$a_m = \rho_{w,i} - \rho_{s,i}$;

$a_e = \rho_{w,i} u_{w,i} - \rho_{s,i} u_{s,i}$;

$b_m = -(w_{wp} + w_{sp})/\phi_f bL$;

$b_e = -(w_{wp}\bar{h}_w + w_{sp}\bar{h}_s)/\phi_f bL$;

$c_m = (\rho_{w,i-1} - \rho_{s,i-1}) z_{l,i-1} + (\rho_{s,i-1} - \rho_{s,i}) z_t + w_r \Delta t_i^{k-1}/\phi_f bL$;

$c_e = (\rho_{w,i-1} u_{w,i-1} - \rho_{s,i-1} u_{s,i-1}) z_{l,i-1} +$
$(\rho_{s,i-1} u_{s,i-1} - \rho_{s,i} u_{s,i}) z_t + \frac{(1-\phi_f)}{\phi_f} \rho_{sR} z_t c_{sR} \cdot$
$\Delta T_i + (w_r h_r + q) \Delta t_i^{k-1}/\phi_f bL$;

where $\bar{h}_w$ and $\bar{h}_s$ are the average enthalpies within a time step for the water and steam phases, respectively.

The water recharge $w_r$ and the heat rate towards the fracture $q$, can be evaluated following the discretization procedure of the convolution integrals presented by Eqs. 9 and 10:

$$w_r(t_i) = \sum_{j=1}^{j=i} \Delta p_j \cdot w_1(\Delta t_i^k + t_{i-1} - t_{j-1}) \quad (9)$$

$$q(t_i) = \sum_{j=1}^{j=i} \Delta T_j \cdot q_1(\Delta t_i^k + t_{i-1} - t_{j-1}) \quad (10)$$

3. Once the following convergence criteria are met

$$|\Delta t_i^k - \Delta t_i^{k-1}| < Tol, \text{ and}$$

$$|z_{l,i}^k - z_{l,i}^{k-1}| < Tol.$$

The new time level $t_i$ is calculated through Eq. 11:

$$t_i = t_{i-1} + \Delta t_i^k. \quad (11)$$

Next the control returns to step 1 of this algorithm and a new time step calculation is started.

After the second time step ($i \geq 3$) the convergence of the algorithm can be speeded up taking into account the results of the two previous time steps. Thus, Eq. 12 can be used for the $\Delta t$ evaluation at the first iteration level ($k = 0$)

$$\Delta t_i^{k=0} = (\frac{t_{i-1} - t_{i-2}}{t_{i-2} - t_{i-3}}) \cdot (t_{i-1} - t_{i-2}) \quad (12)$$

The following criteria were taken for the production of water and/or steam from the fracture:

1. The turbine admission steam rate $w_{s\ adm}$, is considered to be equal to the steam mass production $w_{sp}$ from the fracture steam zone:

$$w_{sp} = w_{s\ adm} \quad (13)$$

2. Fluid production from the water zone $w_{wp}$ occurs under isoenthalpic conditions, resulting in a mixture (water and steam) enthalpy at vapor pressure turbine admission $p_{s\ adm}$, being equal to that of water at fracture pressure (or temperature) conditions $h_w$. Under this assumption the mixture quality at the surface can be expressed as follows:

$$x = \frac{h_w - h_{w\ adm}}{h_{fg\ adm}} \quad (14)$$

where $h_{w\ adm}$ is the water specific enthalpy at turbine admission steam pressure, and $h_{fg\ adm}$ is the latent heat of vaporization.

This study considers a constant turbine admission steam mass rate, $w_{s\ adm}$; thus the water mass production from the fracture can be expressed by Eq. 15:

$$w_{wp} = w_{s\ adm}/x \quad (15)$$

3. For the case of simultaneous mass production from the steam and water zones through a single well, Eqs. 16 and 17 express the steam $w_{sp}$ and water production $w_{wp}$:

$$w_{sp} = f_s w_{s\ adm} \quad (16)$$

$$w_{wp} = f_w(\frac{w_{s\ adm} - w_{sp}}{x}) \quad (17)$$

where $f_s$ and $f_w$ are the liner length fractions in contact with the steam and water phases, respectively.

## PRODUCTION CONDITIONS

It is important to keep in mind that the results of this study to be next presented, were obtained considering a simplified visualization of the system geothermal fracture-recharge-matrix heat source, previously described in relation to Fig. 1.

Table 1 presents the basic data used for the numerical modeling of the ICGF system of this work. As it has been stated, the production conditions considered are of constant turbine admission steam mass rate $w_{s\ adm}$, fixed for our forthcoming results at 1 $kg/s$. The simulations to be discussed are grouped in accordance to the three main physical possibilities that can be present in the field, when dealing with a gas cap reservoir (Grant and Glover, 1984), Fig. 1:

1. Production from the water zone.
2. Production from the steam zone.
3. Mixed production from both zones.

## DISCUSSION OF RESULTS

With regard to case 1 for conditions of the well producing from the steam zone, results are presented in Figs. 2-5. Fig. 2 shows the temperature and pressure variation versus time, observing a decrease of approximately 9.5 $°C$ for a production time of 1300 days. At this time the water level in the fracture reduced to zero, as indicated in Fig. 3. Fig. 4 presents the variation of the recharge mass flow to the fracture versus time; it can be observed that in spite of the high aquifer permeability of 50 Darcys, recharge rates are low in relation to total mass production, in the order of 10 percent. Fig. 5 indicates that the main providing mass source to the steam cap is the evaporation of the water zone, ocurring at its contact with the steam, Fig. 1, with an approximately constant 80 percent of the total production during the considered exploitation period. This finding explains the linear decrease versus time of the water level shown in Fig. 3.

Figs. 6-8 present the results obtained for producing conditions in the water zone. It can be noticed that the producing life of the fracture is substantially reduced, to 215 days. This is due to the fact that a greater mass production from the fracture is needed to provide the specified turbine admission rate of 1 $kg/s$.

Figs. 9 and 10 show the fracture behavior corresponding to case 3 of mixed production from the steam cap and water zone, through a liner open between the 350-400 m fracture height. These graphycal results clearly show two different behaviors of the ICGF, that occur at short and large production times, which correspond to previously discussed cases 1 and 2 with regard to Figs. 2-5 and 6-8, respectively.

Sensitivity studies were also carried out for some of the main parameters that enter into the equations that describe this flow problem. For instance, with regard to the aquifer permeability the values considered were 50,100 and 500 Darcys, resulting in temperature variations essentially coincident. The effect of the thermal conductivity of the matrix surrounding the fracture is presented in Fig. 11, for values of this parameter of 0.0005, 0.0010 and 0.0020 $W/m\ °C$. It can be noticed that its effect is very important, and as expected, increasing the thermal conductivity results in grater heat rates and smaller temperature drops.

One point that deserves discussion is that related to the importance of the steam cap expansion in the thermodynamic behavior of a fracture undergoing exploitation. This significance can be observed when comparing the temperature and pressure behavior versus time for cases 1 and 2, shown in Figs. 2 and 6, observing in the latter results corresponding to production from the liquid zone, a minimum pressure drop due to the high compressibility of steam, that contributes significantly to the pressure support of the system.

TABLE 1. PARAMETERS USED IN THE SIMULATION.

| | |
|---|---|
| Fracture: | |
| $z_t$, $(m)$ | 700 |
| $L$, $(m)$ | 900 |
| $b$, $(m)$ | 0.3 |
| Initial conditions: | |
| $T$, $(°C)$ | 250 |
| $z_l$, $(m)$ | 500 |
| Rock: | |
| $\rho_R = \rho_{sR}$, $(kg/m^3)$ | 2650 |
| $c_R = c_{sR}$, $(kJ/kg\ °C)$ | 1 |
| $\kappa_R = \kappa_{sR}$, $(W/m\ °C)$ | 0.001 |
| Aquifer: | |
| $T_r$, $(°C)$ | 250 |
| $\phi$,( ) | 0.20 |
| $k$, $(Darcy)$ | 50 |
| $c_t$, $(1/Pa)$ | 1.2e-9 |
| Production: | |
| $w_{s\ adm}$, $(kg/s)$ | 1 |
| $p_{s\ adm}$, $(MPa)$ | 0.8 |

## CONCLUSIONS

The main purpose of this paper has been to present results obtained from a numerical solution to a space integrated zero dimensional model (SIZDM), for the description of the thermodynamic behavior of a geothermal fracture undergoing exploitation. The motivation of this work came after identifying the need for a better understanding of the behavior of wells producing from main fractures, in geothermal reservoirs.

From the results of this study, the following conclusions can be made:

1. A SIZDM is presented for the thermodynamic behavior description of a geothermal fracture.
2. The nonlinear equations of mass and energy conservation were numerically solved.
3. The system's behavior is described for exploitation conditions in the steam, in the water, or in both zones.
4. The main providing mass source to the steam cap is the evaporation of the water zone.
5. For producing conditions in the water zone the producing life of the fracture is substantially reduced.
6. The effect of the matrix thermal conductivity on the heat rates is very important.
7. The steam cap expansion has a great significance in the thermodynamic behavior of a fracture.

## NOMENCLATURE

$b$ = fracture thickness $(m)$
$c$ = specific heat $(J/kg\ ^{\circ}C)$
$c_t$ = aquifer total compressibility $(1/Pa)$
$L$ = length of fracture $(m)$
$h$ = specific enthalpy $(J/kg)$
$\bar{h}$ = average specific enthalpy $(J/kg)$
$k$ = permeability $(m^2)$
$\kappa$ = thermal conductivity $(W/m\ ^{\circ}C)$
$p$ = pressure $(Pa)$
$q$ = heat rate toward the fracture $(J/s)$
$q_1$ = influence function $(J/s\ ^{\circ}C)$
$t$ = time $(s)$
$T$ = temperature $(\ ^{\circ}C)$
$u$ = specific internal energy $(J/kg)$
$x$ = mixture quality (fraction)
$z_l$ = liquid level refered to the fracture base $(m)$
$z_t$ = fracture height $(m)$
$z_{l,t=0}$= height of the initial steam-water level $(m)$
$w$ = production $(kg/s)$
$w_1$ = influence function $(kg/sPa)$
$\Delta t$ = time step $(s)$
$\Delta p$ = pressure drop $(= p_i - p_{i-1})$ $(MPa)$
$\Delta T$ = temperature drop $(= T_i - T_{i-1})$ $(\ ^{\circ}C)$
$\rho$ = density $(kg/m^3)$
$\phi$ = porosity (fraction)

**Subscripts:**

$adm$= turbine admission
$f$ = fracture
$i$ = time level
$l$ = liquid
$p$ = production
$r$ = recharge
$R$ = rock
$s$ = steam
$sR$ = solids in the fracture
$w$ = water
1 = influence function

**superscripts:**

$k$ = iteration level

## REFERENCES


Brigham,W.E., and Morrow,C.B. (1977):*P/z Behaviour for Geothermal Steam Reservoirs.* Soc. Pet. Eng. J. **17**(5), pp 407-412.

Brigham, W.E. and Neri, G. (1980): *A Depletion Model for the Gabbro Zone (Northern Part of Larderello Field).* Proc., Second DOE-ENEL Workshop Cooperative Research Geothermal Energy, Berkeley, CA, pp 434-463.

Brownell, D.H., Garg, S.K. and Pritchett, J.W. (1977): *Governing Equations for Gothermal Reservoirs.* Water Resources Research, **13**(6), pp 929-935.

Carslaw, H.S. and Jaeger, J.C. (1959): *Conduction of Heat in Solids.* Oxford University Press, Oxford, England.

Castanier,L.M., Sanyal, S.K. and Brigham, W.E. (1980): *A Practical Analytical Model for Geothermal Reservoir Simulation.* Paper SPE 8887, SPE California Regional Meeting, Los Angeles, CA.

Craft, B.C. and Hawkins, M.F. Jr (1959): *Applied Petroleum Reservoir Engineering.* Prentice-Hall, Inc. New Jersey.

Faust, C.R. and Mercer, J.W. (1979a): *Geothermal Reservoir Simulation, 1. Mathematical Models for Liquid and Vapor Dominated Hydrothermal Systems.* Water Resources Research, **15**(1), pp 23-30.

Faust, C.R. and Mercer, J.W. (1979b): *Geothermal Reservoir Simulation, 2. Mathematical Models for Liquid and Vapor Dominated Hydrothermal Systems.* Water Resources Research, **15**(1), pp 31-46.

Garg, S.K, Pritchett, J.W. and Brownell,D.H. (1975): *Transport of Mass and Energy in Porous Media.* Presented at Second United Nations Symposium on the Development and Use of Geothermal Resources, San Francisco, California, May 20-29.

Garg, S.K., Pritchett, J.W. (1977) : *On Pressure-Work, Viscous Dissipation and the Energy Balance Relation for Geothermal Reservoirs.* Advances in Water Resources, **1**(1), pp 41-47.

Grant, M.A (1977): *Broadlans: A Gas-Dominated Field.* Geothermics, **6**(1), pp 9-29.

Grant, M.A., Donaldson, I.G. and Bixley,P.F. (1982): *Geothermal Reservoir Engineering.* Academic Press, New York.

Muskat,M. (1945):*The Production Histories of Oil Producing Gas-Drive Reservoirs.* Jour. of Applied Physics (March), pp 147-159.

Miller, F.G. (1962): *Theory of Unsteady-State Influx of Water in Linear Reservoir.* Journal of Institute of Petroleum, **48**, pp 365- 379

Nabor, G.W. and Barham, R.H. (1964): *Linear Aquifer Behavior.* May, Jour. Pet. Tech., Trans., AIME, **231**, pp 561-563.

Pruess, K. (1983): *Development of the General Purpose Simulator MULKOM.* Annual Report 1982, Earth Sciences Division, report LBL- 15500, Lawrence Berkeley Laboratory.

Pruess, K. (1987): *TOUGH User's Guide.* Nuclear Regulatory Commission, Report NUREG/CR 4644.

Pruess, K. (1988): *SHAFT, MULKOM, THOUGH: A Set of Numerical Simulators for Multiphase Fluid and Heat Flow.* Geotermia, Revista Mexicana de Geoenergía, **4**(1), pp 185-202.

Raghavan,R. (1994):*Well Test Analysis.* Prentice Hall, Englewood Cliffs, New Jersey.

Schilthuis, R.J. (1936): *Active Oil and Reservoir Energy.* Trans., AIME, **118**, pp 33-52.

Sorey, M.L. and Fradkin, L.J. (1979):*Validation and Comparison of Different Models of the Wairakei Geothermal Reservoir.* Fifth Workshop Geothermal Reservoir Engineering, Stanford University, Stanford, CA, pp 215-220.

Whiting,R.L. and Ramey,H.J. Jr. (1969): *Application of Material and Energy Balances to Geothermal Steam Production.* Jour. of Pet. Tech., July,**21**(7),pp 893-900.


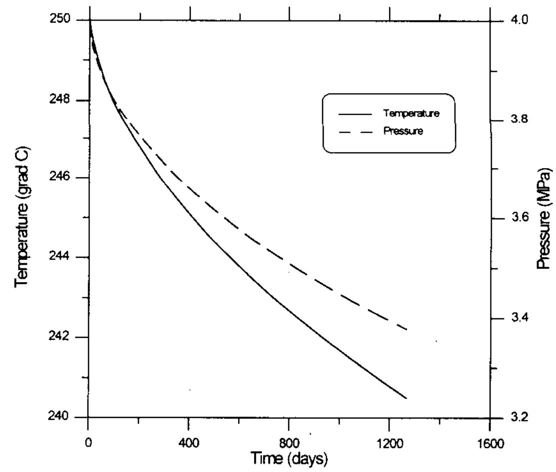


Fig. 2. Temperature and pressure behavior versus time; production from the steam zone.

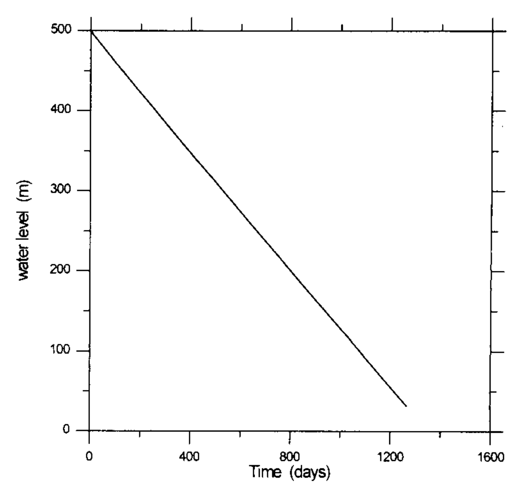


Fig. 3. Water level behavior versus time; production from the steam zone.

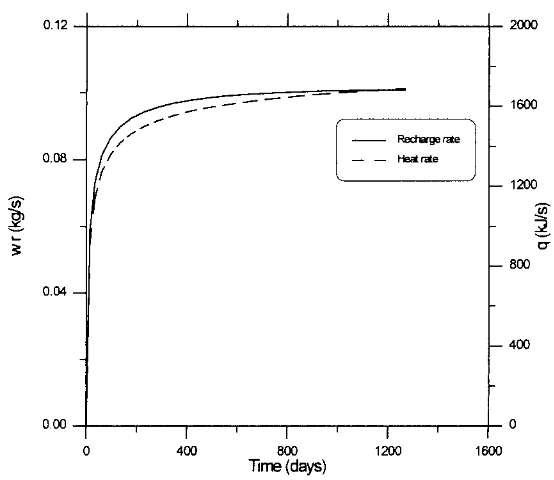


Fig. 4. Water recharge rate and heat rate toward the fracture; production from the steam zone.

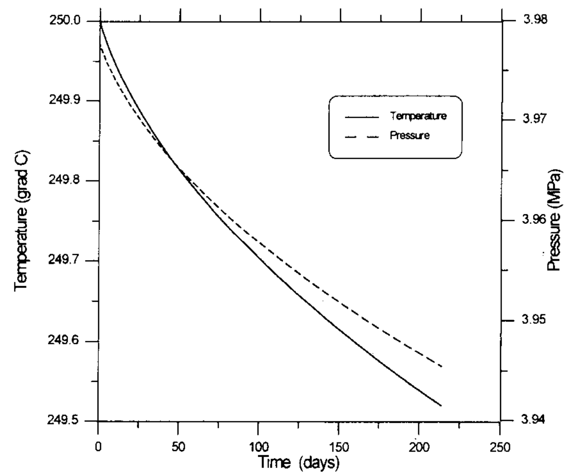


Fig. 6. Temperature and pressure behavior versus time; production from the water zone.

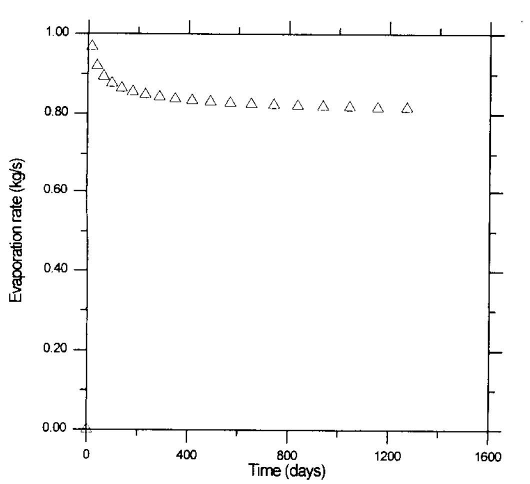


Fig. 5. Evaporation rate of the water zone; production from the steam zone.

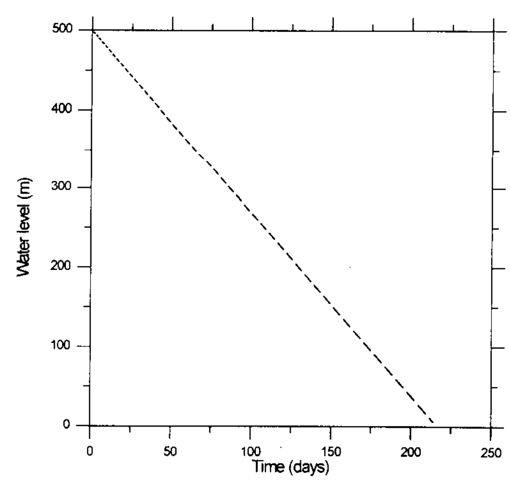


Fig. 7. Water level behavior versus time; production from the water zone.

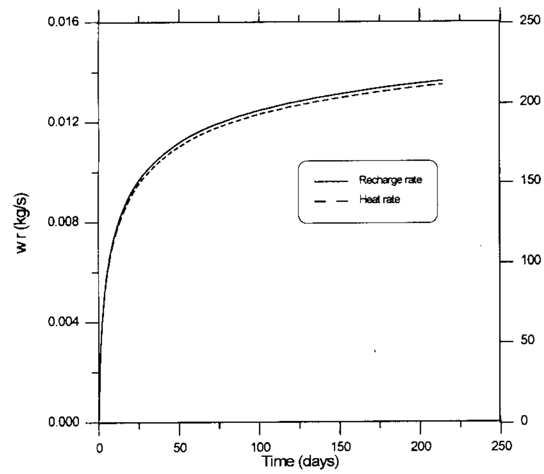


Fig. 8. Water recharge rate and heat rate toward the fracture; production from the water zone.

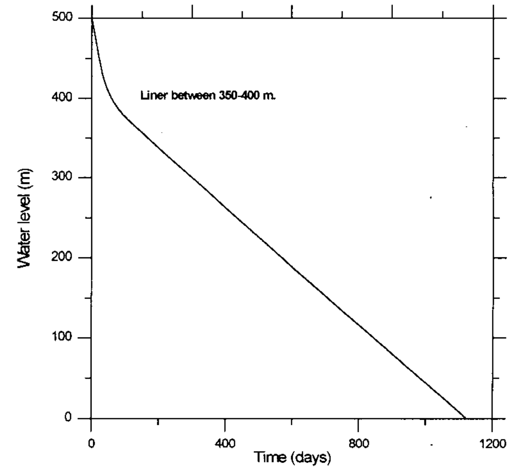


Fig. 10. Water level behavior versus time; mixed production.

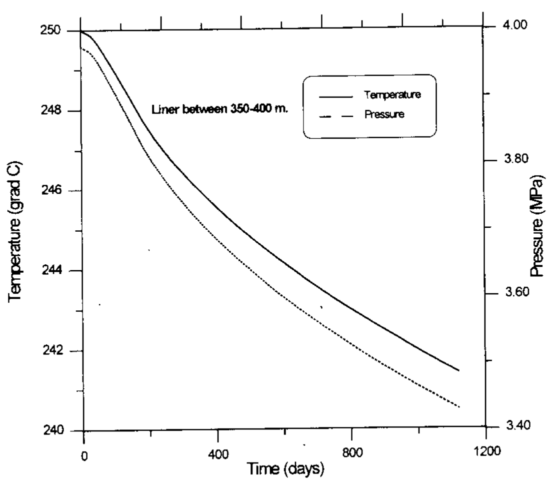


Fig. 9. Temperature and pressure behavior versus time; mixed production.

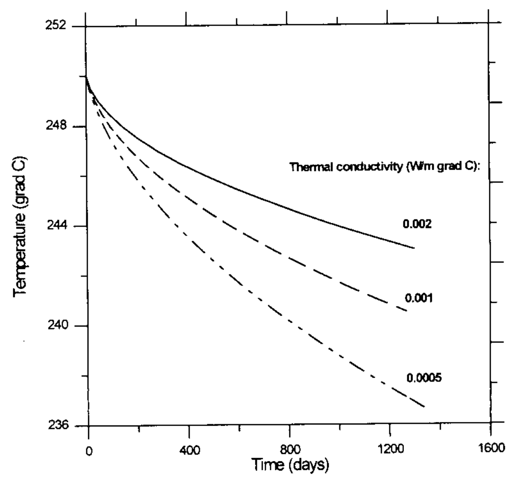


Fig. 11. Effect of the thermal conductivity; production from the steam zone.